SCIENCE CHINA
Chemistry

•ARTICLES•
SPECIAL ISSUE: Celebrating the 100th Anniversary of Chemical Sciences in Nanjing University

May 2020 Vol.63 No.5: 731–740
https://doi.org/10.1007/s11426-020-9712-y

Express and sensitive detection of multiple miRNAs via DNA cascade reactors functionalized photonic crystal array

Yingfei Wang[1], Yuyi Li[1], Yue Zhang[1], Kewei Ren[1,3], Huangxian Ju[1] & Ying Liu[1,2*]

[1]*State Key Laboratory of Analytical Chemistry for Life Science, School of Chemistry and Chemical Engineering, Nanjing University, Nanjing 210023, China;*
[2]*Chemistry and Biomedicine Innovation Center, Nanjing University, Nanjing 210023, China;*
[3]*Department of Chemistry, University of Massachusetts, Amherst, Massachusetts 01003, USA*

Received January 7, 2020; accepted February 24, 2020; published online April 8, 2020

Array based detection techniques with fluorescence signal reading is a powerful tool for multiple targets analysis. However, when applied fluorescence array for microRNA detection, time-consuming multi-steps surface signal amplification is usually required due to the low abundance of microRNA in total RNA expressions, which impairs detection efficiency and limits its application in point of care test (POCT) manner. Herein, DNA cascade reactors (DCRs) functionalized photonic crystal (PC) array was fabricated for express and sensitive detections of miRNA-21 and miRNA-155. DCRs were assembled by interval conjugation of self-quenched hairpin DNA probes to single strand DNA nanowire synthesized by rolling circle amplification, which generated cascade DNA hybridization reactions in response to target miRNA with instant fluorescence recovery signal. PC array patterns with multi-structure colors further amplified fluorescence with their respective photonic bandgaps (PBGs) matching with the emission peaks of fluorescence molecules labelled on DCRs. The as-prepared DCRs functionalized PC array demonstrated express and sensitive simultaneous detections of miRNA-21 and miRNA-155 with hundreds fM detection limits only in 15 min, and was successfully applied in fast quantifications of low abundance miRNAs from cell lysates and spiked miRNAs from human serum, which would hold great potential for disease diagnosis and therapeutic effect monitoring with a POCT manner.

microRNA detection, photonic crystal array, DNA cascade reactors, fluorescence amplification, express detection

Citation: Wang Y, Li Y, Zhang Y, Ren K, Ju H, Liu Y. Express and sensitive detection of multiple miRNAs via DNA cascade reactors functionalized photonic crystal array. *Sci China Chem*, 2020, 63: 731–740, https://doi.org/10.1007/s11426-020-9712-y

1 Introduction

MicroRNAs (miRNAs) are small, endogenous non-coding RNAs with 19–24 nt in length that participate in regulating gene expression after transcription [1–3], as well as maintaining cellular physiological processes [4–6]. Multiple miRNAs work simultaneously and collaboratively in the gene regulatory network [7] during the occurrence and progression of cancers and many diseases such as diabetes, cardiovascular disease and Alzheimer's disease [8,9]. Therefore the joint detections of multiple cancer-specific miRNAs are of great importance for disease early diagnosis and therapeutic effect evaluation. Benefiting from the emerging of various fluorescent dyes and fast advancement in optical imaging [10], fluorescent labeling of targets or detection probes has been widely used to produce signal reading in DNA analysis. Coupling with the cost-effective, easy operated and miniaturized array based detection techniques, miRNAs detection array substrate with fluorescence signal reading has emerged as a powerful tool for high-throughput and multiplex targets analysis with a point of care test (POCT) manner [11].

*Corresponding author (email: yingliu@nju.edu.cn)

Considering the low abundance of miRNA in total RNA expressions, various signal amplification strategies have been coupled with fluorescence substrate to enhance detection sensitivity. MiREIA assay has been developed which used substrate pre-immobilized DNA probes to capture target miRNAs followed by enzymatic reaction for signal amplification [12,13]. Polymerase chain reaction (PCR) [14] and rolling circle amplification (RCA) [15] are commonly used amplification techniques, and have been coupled with array based technique by designing hydrogel microposts fitted in regular qPCR chip [16]. Target triggered nonenzymatic DNA cascade reactions such as hybridization chain reaction (HCR) [17,18] and catalytic hairpin assembly (CHA) [19,20] on substrate resulted the self-assembly of fluorescent DNA detection strands and corresponding effective signal amplification effect [21,22]. Though demonstrating satisfactory detection sensitivity, all the above mentioned signal amplification strategies require time-consuming experiment steps including continuous surface incubation and rinsing, which cost 2–5 h experiment periods [23], making them not appropriate for POCT application. Therefore, the development of multiple miRNAs fluorescence detection array with high sensitivity and express signal obtaining capability is of great significance for the early diagnosis of disease, especially in resource-limited area.

Confining DNA cascade reaction in restricted area significantly enhanced reaction efficiency and detection sensitivity [24–26]. Our group have prepared mRNA responsive DNA cascade reactor (DCR) via DNA self-assembly, which accelerated continuous DNA hybridization reactions and achieved sensitive mRNA detection in homogeneous solution in 15 min [27]. However, when directly applied DCR to biosensing substrate, the high density of surface accumulated fluorophore would result fluorescence self-quenching and therefore impair amplification effect [28,29]. Photonic crystal (PC) is periodic dielectric materials with photonic bandgap (PBG) properties which modulate the propagation of electromagnetic waves [30,31], and light with the same wavelength as PBG cannot propagate through PC correspondingly generate different structure colors with characteristic reflection spectrum [32]. With the emission peak overlapped with the characteristic reflection peak of PC, the fluorescence intensity of surface immobilized fluorophores could be highly amplified [33]. Taking advantages of the property that PBG is proportional to the size of PC component nanoparticles [34,35], here we demonstrated express and sensitive multiple miRNAs detection based on DCRs functionalized PC array with different PBGs. To prepare PC array, a 4×12 array mold was pre-pasted on silanized glass substrate with the subsequent blade coating of a mixture of polyethylene glycol dimethacrylate (PEG-DA-250, MW 250), acrylic acid, photoinitiator and monodispersed silica spheres. Silica spheres with particle size of 250 nm (PC250) and 290 nm (PC290) were chosen as PC component respectively with characteristic reflection peaks at ~575 and ~655 nm. MicroRNA-21 (miRNA-21) and microRNA-155 (miRNA-155), which simultaneously overexpressed in cancer patients at early stage [36,37], were chosen as the model detection targets. To prepare target miRNAs responsive DCRs for accelerated DNA cascade reactions, HCR probe pairs H1 and H2 were pre-conjugated on a single strand DNA nanowire synthesized by rolling circle amplification (RCA). Hairpin structured H1-21 and H1-155 were labelled with fluorescent reporter/corresponding quencher pairs TAMRA/BHQ1 and Cy5/BHQ3 respectively for fluorescence self-quench of DCRs in the absence of target miRNAs. The as-prepared DCRs responsive to miRNA-21 (DCR-21) and miRNA-155 (DCR-155) were then covalently immobilized on PC250 and PC290 respectively to complete the multiple miRNAs express detection array (Scheme 1(a)). In detection process, miRNA-21 and miRNA-155 triggered accelerated HCR in DCRs and resulted the instant fluorescence recovery of TAMRA and Cy5 respectively with prominent signal amplification from substrate PC250 and PC290 (Scheme 1(b)). The as-prepared DCRs functionalized PC array demonstrated express and sensitive detections of miRNA-21 and miRNA-155 with hundreds fM detection limits in 15 min, and were successfully applied in fast quantifications of low abundance miRNAs from cell lysates, which would hold great potential for disease diagnosis and therapeutic effect monitoring in a POCT manner.

2 Experimental

2.1 Materials and reagents

Phi29 DNA polymerase, T4 DNA ligase, exonuclease I, exonuclease III and dNTPs were purchased from New England Biolabs Ltd. (UK). DNA purification kit was obtained from ComWin Biotech Co., Ltd. (China). Acrylic acid, *N*-hydroxysuccinimide (NHS), 1-ethyl-3-[3-dimethylaminopropyl]carbodiimide hydrochloride (EDC•HCl), tetraethyl orthosilicate (TEOS, 98%) and ammonia solution (NH_4OH, 28%–30% NH_3 in water) were purchased from Aladdin Reagent Co., Ltd. (China). 3-Acryloxypropyltrichlorosilane was purchased from Gelest, Inc. (Morrisville, USA). Polyethylene glycol dimethacrylate with molecular weight of 250, 500 and 700 (PEG-DA-250, PEG-DA-500 and PEG-DA-700) and 2-hydroxy-2-methyl-propiophenone (photoinitiator) were purchased from Sigma-Aldrich (USA). The microRNAs were obtained from GenePharma Co., Ltd. (China). All oligonucleotides were synthesized by Sangon Biotech Co., Ltd. (China) with high performance liquid chromatography (HPLC) purification. Sequences of the microRNAs and oligonucleotides were listed in Table S1 (Supporting Information online). Serum from healthy in-

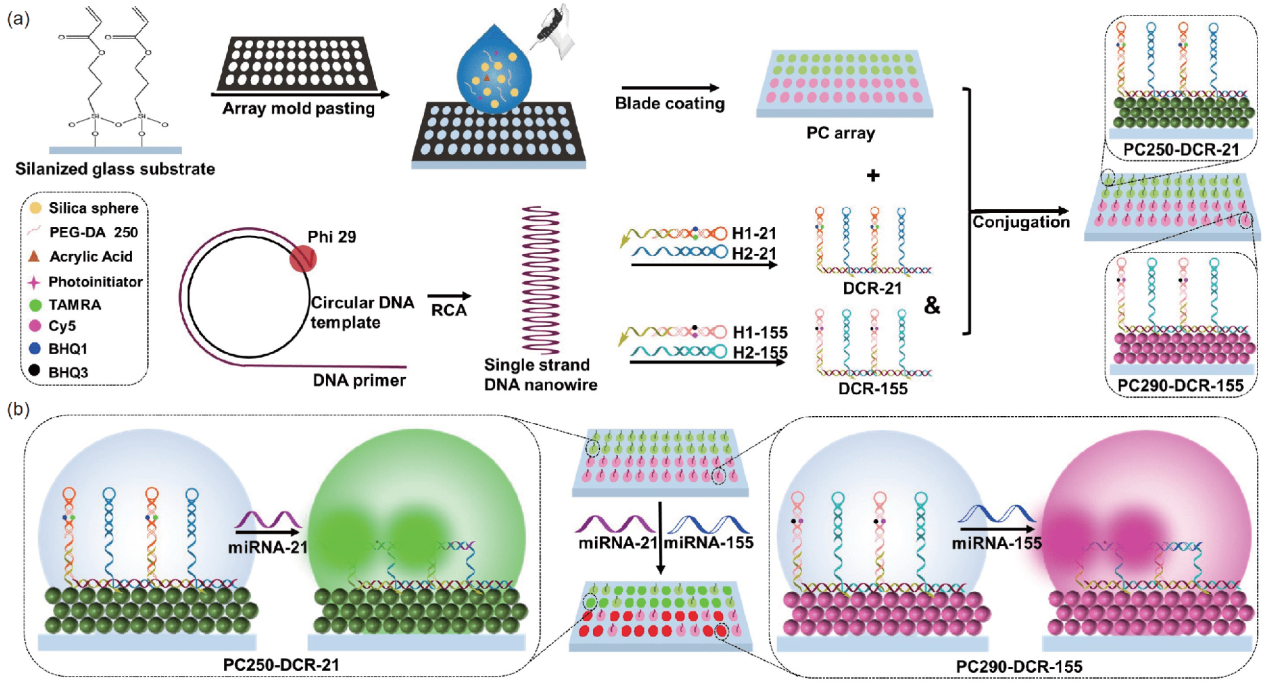

Scheme 1 (a) Schematic illustrations of preparation of DCRs functionalized PC array for multiple miRNAs detection. (b) Instant fluorescence recovery and amplification of TAMRA and Cy5 in response to miRNA-21 and miRNA-155 on DCR-21 functionalized PC250 array patterns (PC250-DCR-21) and DCR-155 functionalized PC290 array patterns (PC290-DCR-155) (color online).

dividuals were from Nanjing Jiangning Hospital. All aqueous solutions were prepared using ultrapure water (≥18 MΩ, Milli-Q, Millipore). Diethy pyrocarbonate (DEPC) treated water was used in the throughout process for miRNA involving operations.

2.2 Apparatus

The gel electrophoresis was performed on PowerPac™ basic electrophoresis analyzer (Bio-Rad, USA) and imaged on Biorad ChemiDoc XRS facility. Fluorescence spectra were measured on a FluoroMax-4 spectrofluorometer (HORIBA Scientific, Japan). Glass slides were cleaned and activated by oxygen plasma cleaner (PDC-MG, Ming Heng, China). The static contact angles were measured with a contact angle system (OCA30, Dataphysic Instruments GmbH, Germany). Scanning electron microscope (SEM) images were obtained by Quattro environmental scanning electron microscope (FEI Company, USA) at 10 kV. TEM images were acquired by Tecnai G2 F20 X-TWIN transmission electron microscope (FEI Company, USA). Reflection spectra were recorded on an UV-3600 UV-Vis-NIR spectrophotometer (Shimadzu Company, Japan). The photonic crystal array was scanned with GenePix 4100A microarray scanner (Molecular Devices, USA) and analysed by GenePix Pro 7 software to obtain corresponding fluorescence intensities. Real-time reverse transcription polymerase chain reaction (RT-PCR) was performed on Applied Biosystems StepOnePlus Real-Time PCR System (ThermoFisher Scientific, USA).

2.3 Synthesis of monodispersed silica spheres

Monodispersed silica spheres were purchased from NanJing Nanorainbow Biotechnology Co., Ltd. (China), which synthesized according to Stöber process as follows [38–40]: 5 mL TEOS was rapidly added into a mixture of 60 mL ethanol, 25 mL H_2O, and 5 mL ammonia, stirred for 2 h followed ethanol rinsing and centrifugation to get SiO_2 spheres with 250 nm in diameter. The size of SiO_2 spheres can be easily adjusted by varying the concentration of ammonia with fixed concentration of TEOS and H_2O.

2.4 Fabrication of PC array

Glass slides (25.4 mm×76.2 mm×1.2 mm) were pretreated by sequentially sonicated in acetone, isopropyl alcohol and DI water, with nitrogen dry before silanization. After treated with oxygen plasma cleaner to activate surface hydroxyl groups [41], the glass substrates were sealed in a preheated desiccator with a piece of filter paper pipetted with 100 μL 3-acryloxypropyltrichlorosilane and 0.5 g $MgSO_4$•$7H_2O$ as water source for hydrolysis reaction. The desiccator was then vacuumed and kept in oven at 80 °C overnight [42] to get the alkene-silanized glass slides. To generate PC array, a PVC mold with 4×12 array of 3 mm in diameter for each pattern size was pasted on the silanized glass slide, 100 μL mixture

solution containing 5% (*m*/*v*) monodispersed silica spheres, 2.4 μL PEG-DA-250, 0.6 μL acrylic acid and 0.3 μL 10% (*v*/*v*) photoinitiator were added on the surface of glass slide, blade coated all patterns evenly and kept under room temperature without disturbance for 2 d. The as-prepared PC array slides were placed in dry condition for further use.

2.5 Functionalization of PC array with DCRs

The DCRs for express cascade DNA hybridization reactions were synthesized by sequentially hybridizing HCR probe pairs H1, H2 to a single strand DNA nanowire prepared by RCA [27]. The circular DNA template for RCA was synthesized by annealing 4.2 μL phosphorylated linear DNA (100 μM) and 4.2 μL ligation DNA (100 μM) at 95 °C for 4 min with slowly cooling to room temperature over 2 h. 1 μL T4 DNA ligase (400 U/μL), 2 μL 10× T4 DNA buffer, and 8.6 μL ultrapure water were then added to the solution and the mixed solution was incubated at 22.5 °C for 16 h followed by enzyme deactivation at 65 °C for 10 min. After treated with 2.5 μL exonuclease I (20 U/μL) and 2.5 μL exonuclease III (100 U/μL) to remove the unreacted linear DNA and ligation DNA, the obtained circular DNA template (10 μL) was mixed with 0.5 μL DNA primer (100 μM) and annealed at 95 °C for 4 min. The reaction mixture was cooled down and incubated with Phi29 DNA polymerase (0.2 U/μL), BSA (0.4 μg/μL), and dNTPs (0.1 mM) at 37 °C for 5 h in 150 μL 1× Phi29 reaction buffer with subsequent heating to 65 °C for 10 min to denature the Phi29 DNA polymerase. The as-obtained single strand DNA nanowire was purified by DNA purification kit and stored in −20 °C.

Self-quenched hairpin1-21 and hairpin1-155 were designed respectively for target miRNA-21 and miRNA-155. H1-21 was synthesized by mixing hairpin1-21 with H1 connector equimolarly reaching a final concentration of 10 μM in phosphate buffer saline (PBS) buffer. The H1 connector was composed of a segment of 24 bases complementary to the 5′-end tail of hairpin1-21 and another segment of 22 bases complementary to the above prepared single strand DNA nanowire for the conjugation of hairpin1-21 to single strand DNA nanowire. H2-21 was composed of a 44 bases hairpin structured segment for hybridization with hairpin1-21 and a 22 bases segment at 3′-end for conjugation to the single strand DNA nanowire. 10 μL H1-21 (10 μM) and 10 μL H2-21 (10 μM) were mixed with 100 μL single strand DNA nanowire, incubated at 37 °C for 2.5 h and purified by ultrafiltration (100,000 MW cutoff membrane, Millipore) for three times to obtain DCR-21 with H1-21 and H2-21 alternatively hybridized on single strand DNA nanowire. The concentration of H1-21 was used as concentration of DNA self-assembled structure. DCR-155 was prepared accordingly with hairpin1-155, H1 connector, and H2-155.

To immobilize the above prepared DCRs on PC array, the carboxyl group of acrylic acid in each PC array pattern was activated by 2.5 μL MES buffer containing 0.4 M EDC and 0.1 M NHS, reacted with 2.5 μL DCRs (100 nM) with subsequent PBS rinsing to remove the excess DCRs.

2.6 Detection of target miRNAs on DCRs functionalized PC array

To establish the calibration curve for miRNA quantification, PC250 array pattern was challenged with miRNA-21 of concentration ranging from 200 fM to 50 nM, while PC290 array pattern was challenged with miRNA-155 with concentration ranging from 100 fM to 50 nM, respectively. After 15 min incubation followed by PBS rinsing, the resulted array patterns were scanned with microarray scanner for fluorescence intensity quantification. General HCRs were also performed on PC250 array patterns as control experiments, which covalently immobilized amine terminus H2*-21 probes on PC array patterns to capture target miRNA-21. After incubation with miRNA-21 and subsequent PBS rinsing, 2.5 μL H1*-21 probes (100 nM) and H2*-21 probes (100 nM) mixture were added in with 15 min incubation with subsequent fluorescence intensity quantification with microarray scanner.

2.7 Polyacrylamide gel electrophoresis (PAGE) analysis

10% Native polyacrylamide gel was prepared using 5× TBE buffer and loaded with 5 μL DNA sample with 1 μL 6× loading buffer. The gel electrophoresis was run at 110 V for 80 min in 1× TBE buffer, and subsequently stained with SYBR™ Gold and scanned with Biorad ChemiDoc XRS facility (Bio-Rad, USA).

2.8 Cell cultrue

Human cervix carcinoma (HeLa) cells (KeyGEN Biotech, China) were cultured at 37 °C in Dulbecco's modified Eagle's medium (DMEM) supplemented with 10% FBS in a humidified incubator containing 5% CO_2 and 95% air. MCF-7 and MCF-10A breast cancer cells (KeyGEN Biotech, Nanjing, China) were cultured in RPMI media 1640 supplemented with 10% FBS at 37 °C in a humidified incubator containing 5% CO_2 and 95% air. Cell numbers were determined with a Petroff-Hausser cell counter (USA).

2.9 Detection of target miRNAs from cell lysate

Cells were rinsed with PBS for three times and processed by a commercial miRNA extraction kit after cell counting. 2.5 μL of the as-prepared cell lysate was incubated with PC

array patterns for expressing signal amplification with subsequent fluorescence quantification by microarray scanner. The obtained fluorescence intensity for each array pattern was substituted into the calibration curve to calculate the corresponding miRNAs concentration in cell lysate which finally converted to copies per cell.

3 Results and discussion

3.1 Fabrication of PC array with multi-structure colors

To fabricate PC array with multi-structure colors, monodispersed silica spheres with respective particle sizes of 250 and 290 nm were synthesized according to Stöber process [38–40] and confirmed by TEM characterization (Figure S1 (a), Supporting Information online). The glass substrate was silanized with 3-acryloxypropyltrichlorosilane, which increased contact angle of glass substrate from ~16° to ~70° (Figure S1(b)). Carboxyl functionalized PC array was then fabricated by blade coating a mixture of PEG-DA, acrylic acid, photoinitiator and monodispersed silica spheres on a 4×12 PVC array mold pre-pasted silanized glass substrate with 3 mm in diameter for each array pattern. The molecular weight of PEG-DA (250, 500, 700) was optimized by mixing with 250 nm monodispersed silica spheres to fabricate PC array respectively. Silica spheres could not assemble into periodic structure with PEG-DA-700 (Figure S2(a)), in accordance with the disappearance of reflection peak in reflection spectrum (Figure S2(b)). To minimize the influence of larger molecular mass PEG-DA on the close packing of silica sphere, PEG-DA-250 was chosen as PC component. With the slow evaporation of water, silica spheres self-assembled into face-centered cubic close-packed structure, while PEG-DA-250 and acrylic acid filled in the space between silica spheres and polymerized under visible light irradiation to endow carboxyl groups to PC array patterns. The successful generation of PC array pattern decreased the contact angle of silanized glass substrate to ~20° (Figure S1 (b)), and the functionalization of carboxyl groups in PC array pattern was confirmed by FTIR spectrum, which demonstrated characteristic peaks at 1729 cm^{-1} for C=O stretching vibration and 1411 cm^{-1} for –COOH bending vibration in accompany with Si–O characteristic peak at 1100 cm^{-1} (Figure 1(a), PC250). The microstructures of PC250 and PC290 patterns demonstrated face-centered cubic closely packed periodic structure in SEM images (Figure 1(b)).

According to the light-matter interactions modulation from the closely packed periodic structure of PC array, the emission of fluorescent molecule attached on PC would be highly enhanced when the emission peak matched with PBG of PC. The PBG wavelength for PC is proportional to the size of component monodispersed silica spheres according to Bragg's equation $\lambda=1.633dn_{average}$, where λ is the PBG wavelength, d is the distance between two adjacent nanoparticles, and $n_{average}$ is the average refractive index. To match PBG wavelength with 580 nm emission peak of TAMRA that labelled on DCR-21, the size of monodispersed silica spheres was optimized from 230 to 260 nm (Figures S3(a), S4(a)), and the correspondingly assembled PC230, PC240, PC250 and PC260 (Figure 1(b) PC250, Figure S4(b)) demonstrated PBGs at 529, 557, 575 and 598 nm, respectively (Figure S3(b)). PC250, with the perfect overlap of PBG at 575 nm with TAMRA emission peak (Figure 1(c) and Figure S3(b)), demonstrated the highest enhancement of ~22.5-fold for TAMRA fluorescence intensity (Figure S3). Therefore, monodispersed silica spheres with 250 nm in diameter was chosen to assemble PC pattern for TAMRA fluorescence enhancement. Considering PBG (λ) of 575 nm and silica

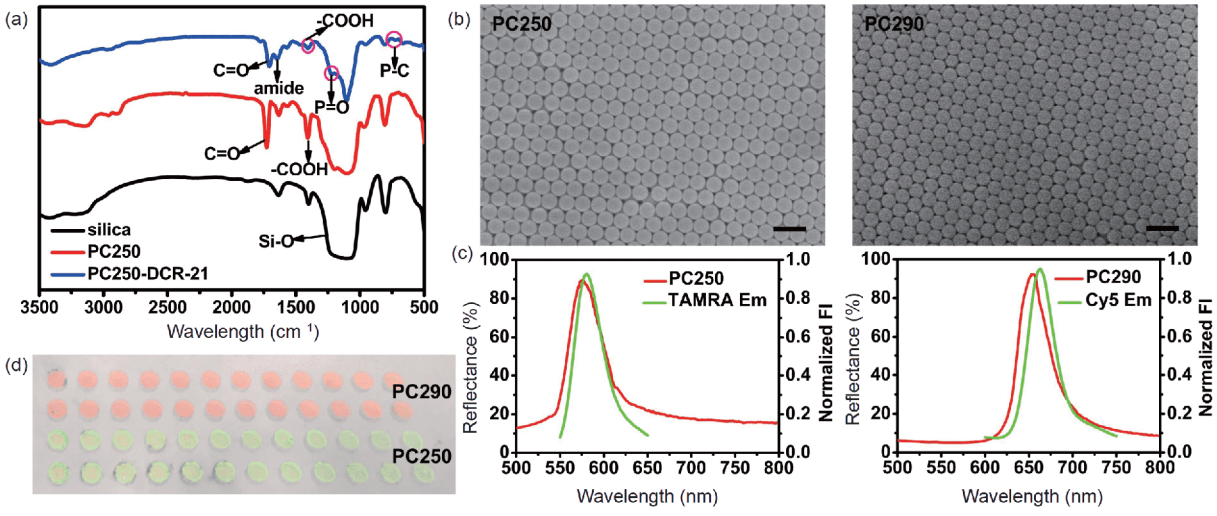

Figure 1 Characterization of PC array. (a) FTIR spectra of silica spheres, PC250, and DCR-21 functionalized PC250 (PC250-DCR-21). (b) SEM images of PC250 and PC290. Scale bar: 500 nm. (c) PBGs of PC250, PC290 and fluorescence emission spectra of TAMRA, Cy5. (d) Photograph of PC250 and PC290 array patterns on silanized glass substrate (color online).

particle size (d) of 250 nm, $n_{average}$ was calculated as 1.41 according to Bragg's equation. With PBG wavelength similar to Cy5 emission peak at 663 nm, the component silica spheres size of PC pattern was calculated as 290 nm for highest fluorescence enhancement factor of Cy5. PBG of as-prepared PC290 was measured at 655 nm in reflection spectrum, which matched well with the emission wavelength of Cy5 (Figure 1(c)). The as-prepared PC250 and PC290 array patterns showed green and red color respectively under daylight exposure (Figure 1(d)).

3.2 Functionalization of PC array with DNA cascade reactors

DCRs were prepared according to our previously reported approach [27] by assembling hairpin structured HCR probes H1/H2 with single strand DNA nanowire synthesized by RCA. H1 was composed of H1 connector which hybridized to single strand DNA nanowire and self-quenched hairpin1. H1-21 was labelled with TAMRA and its corresponding quencher BHQ1 in proximate locations with closed hairpin structure to generate TAMRA fluorescence self-quenched DCR-21, and H1-155 was labelled with Cy5 and its corresponding quencher BHQ3 to generate Cy5 fluorescence self-quenched DCR-155. The synthesis of DCR-21 was confirmed by polyacrylamide gel electrophoresis (PAGE) analysis (Figure 2(a)). The single strand DNA nanowire generated via RCA showed a bright band with wide base distribution around 700 bp (lane 3, Figure 2(a)). After incubating single strand DNA nanowire with H1-21 (lane 1, Figure 2(a)) and H2-21 (lane 2, Figure 2(a)), both H1-21 and H2-21 bands were disappeared, accompanied with the appearance of an extended band with lower mobility (lane 4, Figure 2(a)), indicating the successful synthesis of DCR-21. Atom force microscopy (AFM) characterization of DCR-21 demonstrated monodispersed rigid structure with an average length of 300±50 nm (Figure 2(b)) and height of ~2 nm (Figure 2(c)). Given that H1 connector and H2-21 conjugation parts were both 22 bases individually (~7.48 nm), DCR-21 was calculated to contain 20±3 pairs of H1-21/H2-21. DCR-155 was prepared accordingly with H1-155/H2-155 pairs, and showed bright band with similar base pair number as DCR-21 in PAGE (lane 5, Figure 2(a)).

Due to the proximate locations and alternate arrangement of HCR probe pairs in DCRs, the single strand DNA nanowire accelerated the successive hybridizations of HCR probe pairs efficiently and resulted the continuous opening of hairpin structured H1 with intense fluorescence recovery for fast and sensitive detection. The reaction feasibility of DCRs to target miRNAs was first verified in homogeneous solution. DCR-21 and DCR-155 was incubated with their corresponding target miRNA with concentrations ranging from 1 pM to 100 nM for 15 min, which demonstrated obvious

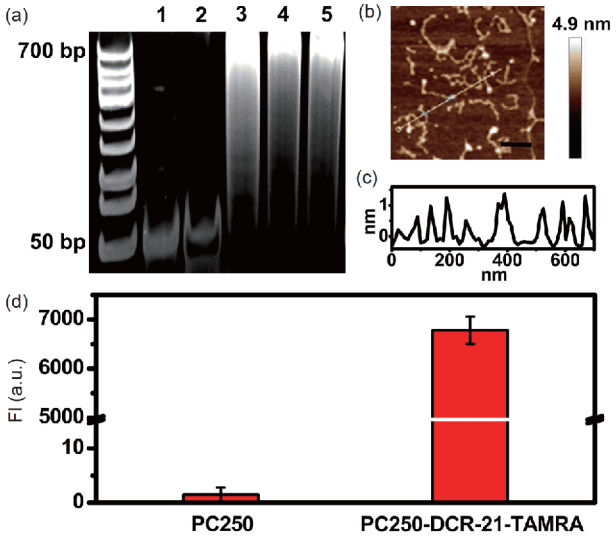

Figure 2 (a) PAGE analysis of DCRs assembly. Lanes 1–5 represent H1-21, H2-21, single strand DNA nanowire, DCR-21 and DCR-155. (b) AFM phase image of DCR-21 and (c) cross-section profile of the white line in (b). Scale bar: 200 nm. (d) Fluorescence intensities at 580 nm for PC250 array pattern and DCR-21-TAMRA functionalized PC250 (PC250-DCR-21-TAMRA) array pattern. The error bars indicate means±S.D. (n=4) (color online).

fluorescence recoveries for TAMRA at 580 nm and Cy5 at 663 nm, respectively even at low concentration of 1 pM (Figure S5 (a, c)). A linear range for the logarithmic value of miRNA-21 concentration from 10 pM to 5 nM was obtained with detection limit of 6.36 pM (Figure S5(b)) and a linear range for the logarithmic value of miRNA-155 concentration from 20 pM to 20 nM with detection limit of 13.34 pM (Figure S5(d)). To demonstrate the reaction efficiency in DCRs, 5 nM miRNA-21 was incubated with 100 nM DCR-21, and the time-dependent fluorescence recovery of TAMRA at 580 nm was measured for 2 h, which showed substantial fluorescence intensity increase in very short time and reached signal saturation only in 15 min (Figure S6(a)) with 5.8 folds fluorescence intensity enhancement compared with that from DCR-21 in the absence of miRNA-21 (Figure S6 (b)). In comparison, traditional HCR was also performed by mixing 5 nM miRNA-21 with 100 nM H1*-21 and H2*-21, which took more than 2 h for fluorescence recovery saturation (Figure S6(a)) with only 3 folds of fluorescence intensity enhancement after 15 min compared with the situation in the absence of miRNA-21 (Figure S6(b)). DCR confined reaction area by arranging HCR probe pairs along single strand DNA nanowire alternatively, which increased the collision frequency between HCR probe pairs and resulted express signal generation with largely shortened reaction time.

The as-prepared DCRs were covalently immobilized on carboxylated PC array patterns with H1 terminus amine functional groups, and demonstrated characteristic peaks for amide bond at 1643 cm^{-1} for N–H bending vibration, and 1708 cm^{-1} for C=O stretching vibration in FTIR spectrum, in

accompany with the decrease of carboxyl stretching vibration peak at 1411 cm^{-1}. Meanwhile, the characteristic peaks for phosphate backbone of DNA showed up at 1220 cm^{-1} for P=O stretching vibration and 770–650 cm^{-1} for P–C vibration (Figure 1(a), PC250-DCR-21), confirming the covalent conjugation of DCRs to PC array pattern. To further confirm the immobilization of DCRs to PC array pattern, hairpin1-21-TAMRA was used to compose DCRs instead of self-quenched haripin1-21, and the as-prepared DCR-21-TAMRA was incubated with carboxylated PC250 array pattern, which showed strong fluorescence at 580 nm compared to PC250 array pattern in the absence of DCR-21-TAMRA with negligible fluorescence (Figure 2(d)).

3.3 MiRNA-21 and miRNA-155 detection on DNA cascade reactors functionalized PC array

To confirm the express and sensitive detection of miRNAs on DCRs functionalized PC array, a series concentrations of miRNA-21 were incubated with DCR-21 functionalized PC250 array patterns for 15 min before fluorescence measurement of each array pattern with GenePix scanner. MiRNA-21 triggered the successive opening of H1-21 with the isolation of TRAMA and BHQ1 for fluorescence recovery of TRAMA, which was instantly amplified by PC250 array pattern (Figure 3(a)). The scanned images of miRNA-21 incubated DCR-21 functionalized PC250 array patterns became brighter with miRNA-21 concentration increase, and the fluorescence intensity of array pattern at 580 nm demonstrated a linear relationship versus the logarithmic value of miRNRA-21 concentration from 200 fM to 10 nM with the detection limit of 191.33 fM (Figure 3(a)). The detection limit of the presented DCRs functionalized PC array was comparable to most fluorescence biosensing approaches with signal amplification strategies [9,21,43] with shortest reaction time for express signal acquistion. To demonstrate the contribution of PC array to fluorescence enhancement, PEGDA-250, acrylic acid and photointitiator (10%, *v*/*v*) were mixed in the absence of monodispersed silica spheres and polymerized on silanized glass substrate with the subsequent surface immobilization of DCR-21, the as-obtained DCR-21 functionalized glass substrate was challenged with various concentrations of miRNA-21, which barely showed fluorescence below 20 pM (Figure S7(a)). Another control experiment was performed by immobilizing 100 nM H2*-21 with amine functional group to PC250 array patterns for target miRNA-21 capture. After surface rinsing to remove nonspecific adsorbed miRNA-21, homogeneous HCR signal amplification was performed on substrate with a mixture of 100 nM H1*-21 and H2*-21, which barely showed fluorescence with miRNA-21 concentration below 10 pM (Figure S7(b)). To further demonstrate the acceleration effect from DCR-21, 10 nM miRNA-21 was incubated with PC250 array patterns, and the fluorescence recovery of TRAMA from homogeneous HCR amplification was scanned periodically for 4 h. 10 nM miRNA-21 only resulted 4.9 folds fluorescence signal enhancement after 15 min reaction, and the signal enhancement factor saturated at 7.6 after 4 h reaction (Figure 3(b)). In comparison, 10 nM miRNA-21 resulted ~12 folds of signal enhancement on DCR-21 functionalized PC250 array only within 15 min incubation (Figure 3(b)). The detection of miRNA-21 demonstrated a linear range from 20 pM to 10 nM with detection limit of 15.20 pM on DCR-21 functionalized glass substrate (Figure S7(a)), and a linear range of 10 pM to 5 nM with detection limit of 8.50 pM for homogeneous HCR on PC250 array (Figure S7(b)). The DCR-21 functionalized PC250 efficiently pushed down miRNA-21 detection limit by ~44-fold compared with regular HCR amplification strategy on PC250 and ~79-fold compared with DCR-21 functionalized glass slide (Figure 3(c)), confirming the impressive capability of DCR functionalized PC array for express and sensitive detection.

To extend the application of DCRs functionalized PC array for multiple miRNAs detection, DCR-155 was covalently immobilized on PC290 array patterns, and challenged with various concentrations of miRNA-155, which also demonstrated linear increase of Cy5 fluorescence at 663 nm versus the logarithmic value of miRNA-155 concentrations from 500 fM to 10 nM with detection limit of 265.76 fM (Figure 4(a, b)). The reaction specificity was further tested by measuring TRAMA fluorescence recovery from DCR-21 functionalized PC250 array patterns and Cy5 fluorescence recovery from DCR-155 functionalized PC290 array patterns in response to 10 nM miRNA-21, miRNA-155, nonspecific miRNA-199a and miRNA-141, and corresponding target miRNAs with 3-mismatched bases and 1-mismatched base (3-mismatched miRNA-21 and 1-mismatched miRNA-21 for DCR-21 functionalized PC250 array, and 3-mismatched miRNA-155 and 1-mismatched miRNA-155 for DCR-155 functionalized PC290 array), which demonstrated obvious TRAMA and Cy5 fluorescence recoveries for corresponding target miRNAs with negligible fluorescence recovery for nonspecific miRNAs and 3-mismatched miRNAs, with much lower fluorescence recoveries for 1-mismatched miRNAs compared with those of corresponding target miRNAs (Figure 4(c)). The good reaction specificity allows the application of DCRs functionalized PC array for multiplexed detection of miRNAs in real samples.

3.4 Simultaneous detection of miRNA-21 and miRNA-155 from cell lysates

Due to the impressive biosensing performance of DCRs functionalized PC array, it was applied to determine the expression level of miRNA-21 and miRNA-155 from cell lysates. MiRNA-21 inhibitor and miRNA-155 inhibitor were

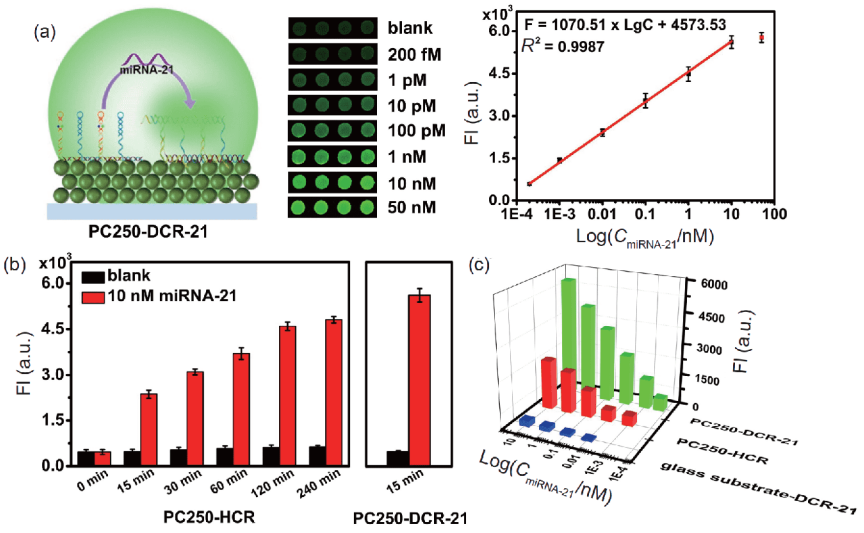

Figure 3 (a) Fluorescence images at 580 nm and calibration curve of DCR-21 functionalized PC250 array patterns (PC250-DCR-21) in response to 200 fM–50 nM miRNA-21. (b) Time-dependent fluorescence recovery of TAMRA for homogeneous HCR on PC250 (PC250-HCR) and fluorescence recovery of TAMRA for PC250-DCR-21 after 15 min reaction in response to 10 nM miRNA-21. (c) Comparison of fluorescence intensities at 580 nm for PC250-DCR-21, PC250-HCR, and DCR-21 functionalized glass substrate (glass substrate-DCR-21) in response to 200 fM, 1 pM, 10 pM, 100 pM, 1 nM and 10 nM miRNA-21. The error bars indicate means±S.D. (n=4) (color online).

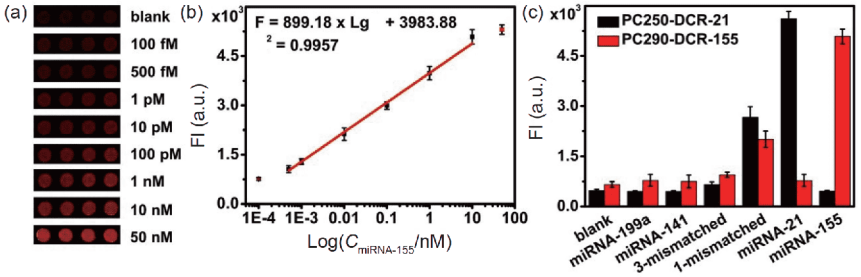

Figure 4 (a) Fluorescence images of DCR-155 functionalized PC290 (PC290-DCR-155) with various concentration of miRNA-155 ranging from 100 fM to 50 nM. (b) Linear relationship of fluorescence intensity versus logarithm of miRNA-155 concentration. (c) Specificity and cross-reaction investigation of DCR-21 functionalized PC250 array (PC250-DCR-21) and PC290-DCR-155 in response to 10 nM miRNA-21, miRNA-155, noncomplementary miRNA-141 and miRNA-199a, and corresponding target miRNAs with 3-mismatched bases and 1-mismatched base. The error bars indicate means±S.D. (n=4) (color online).

transfected into human cervix carcinoma (HeLa) cells respectively to modulate intracellular miRNAs expressions, and the lysates from 10^5 treated HeLa cells were incubated with DCR-21 functionalized PC250 and DCR-155 functionalized PC290 array patterns for miRNA-21 and miRNA-155 detection. Meanwhile, RT-PCR was employed to validate the transfection accuracy by means of miRNA-21 and miRNA-155 calibration curves with a linear range of 20 fM–2 nM (Figure S8). Compared with the fluorescence from untreated HeLa cell lysates, miRNA-21 inhibitor transfected HeLa cell lysates demonstrated lower TAMRA fluorescence from DCR-21 functionalized PC250 array patterns, while the Cy5 fluorescence from DCR-155 functionalized PC290 array patterns showed negligible changes. MiRNA-155 inhibitor transfected HeLa cell lysates demonstrated lower Cy5 fluorescence from DCR-155 functionalized PC290 array patterns, while the TAMRA fluorescence from DCR-21 functionalized PC250 array patterns showed negligible changes (Figure 5(a)). Both miRNA-21 and miRNA-155 expression levels were evaluated from DCRs functionalized PC array according to calibration curves from Figures 3(a), 4(b), and converted to the copy number of miRNAs per cell, which basically agreed with those measured by RT-PCR (Figure 5(b), Figure S9(a)). The lysates from 10^5 cells of MCF-7 cells and MCF-10A cells were also analyzed with DCRs functionalized PC array (Figure S9(b)), and converted to copy number of miRNA-21 and miRNA-155 per cell, which were in full agreement with those measured by RT-PCR (Figure 5(c), Figure S9(c)). The tendency of target microRNAs expression difference in MCF-7, MCF-10A and HeLa cells was in good accordance with previously reported measurements [29,44], indicating the high detection accuracy of DCRs functionalized PC array in cell lysates analysis.

Recovery experiments were further applied to analyse the concentration of target miRNAs spiked in human serum.

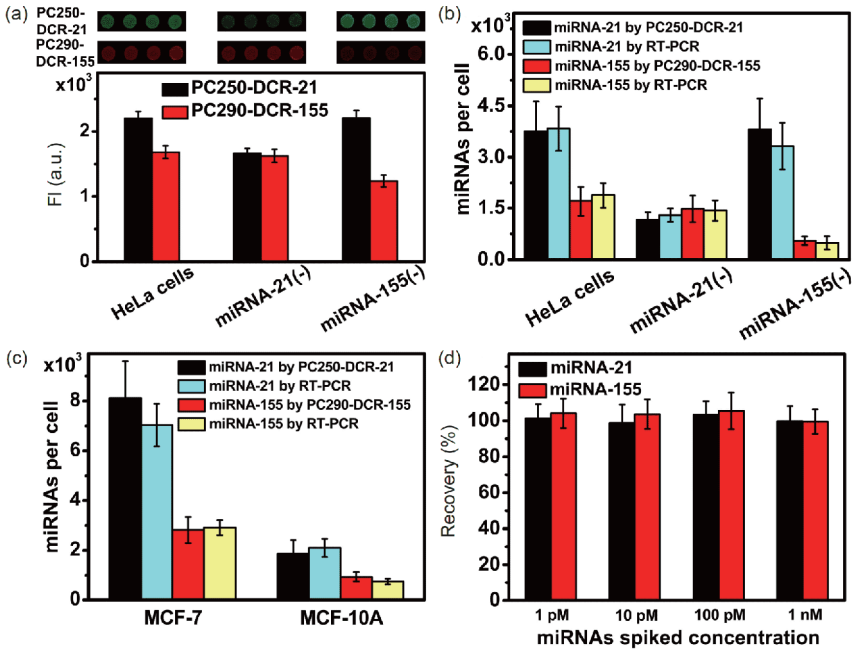

Figure 5 (a) Fluorescence intensities of TAMRA from DCR-21 functionalized PC250 array patterns (PC250-DCR-21) and Cy5 from DCR-155 functionalized PC290 array patterns (PC290-DCR-155) for HeLa cells, miRNA-21 inhibitor treated HeLa cells (miRNA-21(−)), and miRNA-155 inhibitor treated HeLa cells (miRNA-155(−)) (inset: corresponding fluorescence images). Average miRNA-21 and miRNA-155 copy number per cell for HeLa cells, miRNA-21 inhibitor treated HeLa cells (miRNA-21(−)), miRNA-155 inhibitor treated HeLa cells (miRNA-155(−)) (b) and MCF-7, MCF-10A cells determined with DCRs functionalized PC array and RT-PCR (c). (d) Recovery rate of diverse concentrations of miRNAs spiked in 10× diluted human serum (color online).

Various amounts of miRNA-21 and miRNA-155 were spiked into 10× diluted serum from healthy individuals with terminal concentration of 1 pM, 10 pM, 100 pM, and 1 nM, and analysed with DCRs functionalized PC array, which showed less than 10% of relative standard deviation (RSD) and more than 90% of recovery rate (Figure 5(d)), indicating the potential application of DCRs functionalized PC array in clinical analysis and diagnosis.

4 Conclusions

In summary, we developed a DCRs functionalized PC array for express and sensitive detection of miRNA-21 and miRNA-155 with detection limits of 191.33 and 265.76 fM, respectively. DCRs with confined structure accelerated the signal amplification process of cascade DNA hybridization reactions from over hours to 15 min, and the substrate PC array patterns further amplified fluorescence intensity with respective PBGs matching with the emission peaks of fluorescent molecules labelled on DCRs. MiRNA-21 and miRNA-155 from cell lysates and spiked miRNAs from human serum were determined, and the results were consistent well with those obtained from RT-PCR. The method provides a universal platform for express and sensitive miRNAs sensing with a POCT manner, thus has promising potential in clinical diagnosis and therapeutic effect evaluation.

Acknowledgements This work was supported by the National Natural Science Foundation of China (21635005, 21605083, 21974064), the National Research Foundation for Thousand Youth Talents Plan of China, Specially-appointed Professor Foundation of Jiangsu Province, and Program for innovative Talents and Entrepreneurs of Jiangsu Province.

Conflict of interest The authors declare that they have no conflict of interest.

Supporting information The supporting information is available online at http://chem.scichina.com and http://link.springer.com/journal/11426. The supporting materials are published as submitted, without typesetting or editing. The responsibility for scientific accuracy and content remains entirely with the authors.

1 Bushati N, Cohen SM. *Annu Rev Cell Dev Biol*, 2007, 23: 175–205
2 Filipowicz W, Bhattacharyya SN, Sonenberg N. *Nat Rev Genet*, 2008, 9: 102–114
3 Guo H, Ingolia NT, Weissman JS, Bartel DP. *Nature*, 2010, 466: 835–840
4 Baek D, Villén J, Shin C, Camargo FD, Gygi SP, Bartel DP. *Nature*, 2008, 455: 64–71
5 Croce CM. *Nat Rev Genet*, 2009, 10: 704–714
6 Krol J, Loedige I, Filipowicz W. *Nat Rev Genet*, 2010, 11: 597–610
7 Lu Y, Zhao X, Liu Q, Li C, Graves-Deal R, Cao Z, Singh B, Franklin JL, Wang J, Hu H, Wei T, Yang M, Yeatman TJ, Lee E, Saito-Diaz K, Hinger S, Patton JG, Chung CH, Emmrich S, Klusmann JH, Fan D, Coffey RJ. *Nat Med*, 2017, 23: 1331–1341
8 Small EM, Olson EN. *Nature*, 2011, 469: 336–342
9 Pasquardini L, Potrich C, Vaghi V, Lunelli L, Frascella F, Descrovi E, Pirri CF, Pederzolli C. *Talanta*, 2016, 150: 699–704
10 Wang C, Li Z. *Mater Chem Front*, 2017, 1: 2174–2194
11 Xue Q, Kong Y, Wang H, Jiang W. *Chem Commun*, 2017, 53: 10772–10775
12 Stejskal D, Hlozankova M, Sigutova R, Andelova K, Svagera Z,

Svestak M. *Biomed Pap Med Fac Univ Palacky Olomouc Czech Repub*, 2019, 163: 39–44
13 Krepelkova I, Mrackova T, Izakova J, Dvorakova B, Chalupova L, Mikulik R, Slaby O, Bartos M, Ruzicka V. *Biotechniques*, 2019, 66: 277–284
14 Benes V, Castoldi M. *Methods*, 2010, 50: 244–249
15 Cheng Y, Zhang X, Li Z, Jiao X, Wang Y, Zhang Y. *Angew Chem Int Ed*, 2009, 48: 3268–3272
16 Choi W, Yeom SY, Kim J, Jung S, Jung S, Shim TS, Kim SK, Kang JY, Lee SH, Cho IJ, Choi J, Choi N. *Biosens Bioelectron*, 2018, 101: 235–244
17 Dirks RM, Pierce NA. *Proc Natl Acad Sci USA*, 2004, 101: 15275–15278
18 Bi S, Yue S, Zhang S. *Chem Soc Rev*, 2017, 46: 4281–4298
19 Li X, Yao D, Zhou J, Zhou X, Sun X, Wei B, Li C, Zheng B, Liang H. *Sci China Chem*, 2020, 63: 92–98
20 Chen J, Liu B, Song X, Tong P, Yang H, Zhang L. *Sci China Chem*, 2015, 58: 1906–1911
21 Chao J, Li Z, Li J, Peng H, Su S, Li Q, Zhu C, Zuo X, Song S, Wang L, Wang L. *Biosens Bioelectron*, 2016, 81: 92–96
22 Yin F, Liu H, Li Q, Gao X, Yin Y, Liu D. *Anal Chem*, 2016, 88: 4600–4604
23 Yao Q, Wang Y, Wang J, Chen S, Liu H, Jiang Z, Zhang X, Liu S, Yuan Q, Zhou X. *ACS Nano*, 2018, 12: 6777–6783
24 Wei Q, Huang J, Li J, Wang J, Yang X, Liu J, Wang K. *Chem Sci*, 2018, 9: 7802–7808
25 Ren K, Zhang Y, Zhang X, Liu Y, Yang M, Ju H. *ACS Nano*, 2018, 12: 10797–10806
26 Zhu X, Ye H, Liu JW, Yu RQ, Jiang JH. *Anal Chem*, 2018, 90: 13188–13192
27 Ren K, Xu Y, Liu Y, Yang M, Ju H. *ACS Nano*, 2018, 12: 263–271
28 Hou J, Zhang H, Yang Q, Li M, Song Y, Jiang L. *Angew Chem Int Ed*, 2014, 53: 5791–5795
29 Wu L, Wang Y, He R, Zhang Y, He Y, Wang C, Lu Z, Liu Y, Ju H. *Anal Chim Acta*, 2019, 1080: 206–214
30 Zhao Y, Zhao X, Gu Z. *Adv Funct Mater*, 2010, 20: 2970–2988
31 Ye XZ, Qi LM. *Sci China Chem*, 2014, 57: 58–69
32 Zhao Y, Xie Z, Gu H, Zhu C, Gu Z. *Chem Soc Rev*, 2012, 41: 3297–3317
33 Fenzl C, Hirsch T, Wolfbeis OS. *Angew Chem Int Ed*, 2014, 53: 3318–3335
34 Bian F, Wu J, Wang H, Sun L, Shao C, Wang Y, Li Z, Wang X, Zhao Y. *Small*, 2018, 14: 1803551
35 Wang Y, Shang L, Bian F, Zhang X, Wang S, Zhou M, Zhao Y. *Small*, 2019, 15: 1900056
36 Iorio MV, Ferracin M, Liu CG, Veronese A, Spizzo R, Sabbioni S, Magri E, Pedriali M, Fabbri M, Campiglio M, Ménard S, Palazzo JP, Rosenberg A, Musiani P, Volinia S, Nenci I, Calin GA, Querzoli P, Negrini M, Croce CM. *Cancer Res*, 2005, 65: 7065–7070
37 Jemal A, Siegel R, Ward E, et al. Cancer statistics, 2009. *CA: a cancer journal for clinicians*, 2009, 59(4): 225-249
38 Wang W, Gu B, Liang L, Hamilton W. *J Phys Chem B*, 2003, 107: 3400–3404
39 Zhang T, Zhang Q, Ge J, Goebl J, Sun M, Yan Y, Liu Y, Chang C, Guo J, Yin Y. *J Phys Chem C*, 2009, 113: 3168–3175
40 Luo Z, Hong RY, Xie HD, Feng WG. *Powder Tech*, 2012, 218: 23–30
41 Seo JH, Shin DS, Mukundan P, Revzin A. *Colloids Surfs B-Biointerfaces*, 2012, 98: 1–6
42 Meng X, Hu J, Chao Z, Liu Y, Ju H, Cheng Q. *ACS Appl Mater Interfaces*, 2018, 10: 1324–1333
43 Pei X, Yin H, Lai T, Zhang J, Liu F, Xu X, Li N. *Anal Chem*, 2018, 90: 1376–1383
44 Liu Q, Wang D, Yuan M, He BF, Li J, Mao C, Wang GS, Qian H. *Chem Sci*, 2018, 9: 7562–7568